AD-A165 575 GRAVITY GRADIOMETER SURVEY ERRORS(U) ANALYTIC SCIENCES 1/1
CORP READING MA S J BRZEZOWSKI MAR 85 TASC-TR-4423-3
AFGL-TR-85-0066

UNCLASSIFIED F/G 8/5 NL

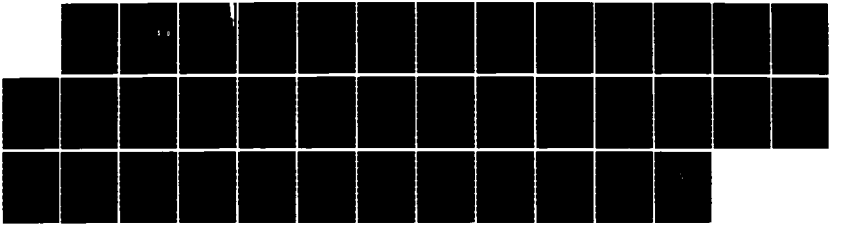

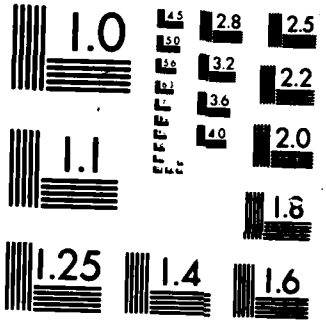

AFGL-TR-85-0066

GRAVITY GRADIOMETER SURVEY ERRORS

STEVEN J. BRZEZOWSKI

THE ANALYTIC SCIENCES CORPORATION
One Jacob Way
Reading, MA 01867

MARCH 1985

SCIENTIFIC REPORT NO. 4

Approved for public release; distribution unlimited

Prepared for:

AIR FORCE GEOPHYSICS LABORATORY
AIR FORCE SYSTEMS COMMAND
UNITED STATES AIR FORCE
HANSCOM AFB, MASSACHUSETTS 01731

CONTRACTOR REPORTS

This technical report has been reviewed and is approved for publication.

Donna Warner

DONNA WARNER
Contract Manager

THOMAS P. ROONEY
Chief, Geodesy & Gravity Branch

FOR THE COMMANDER

Donald H. Eckhardt

DONALD H. ECKHARDT
Director
Earth Sciences Division

This report has been reviewed by the ESD Public Affairs Office (PA) and is releasable to the National Technical Information Service (NTIS).

Qualified requesters may obtain additional copies from the Defense Technical Information Center. All others should apply to the National Technical Information Service.

If your address has changed, or if you wish to be removed from the mailing list, or if the addressee is no longer employed by your organization, please notify AFGL/DAA, Hanscom AFB, MA 01731. This will assist us in maintaining a current mailing list.

UNCLASSIFIED
SECURITY CLASSIFICATION OF THIS PAGE

REPORT DOCUMENTATION PAGE

Form Approved
OMB No. 0704-0188
Exp. Date: Jun 30, 1986

1a. REPORT SECURITY CLASSIFICATION: Unclassified	1b. RESTRICTIVE MARKINGS: None
2a. SECURITY CLASSIFICATION AUTHORITY: N/A	3. DISTRIBUTION/AVAILABILITY OF REPORT: Approved for Public Release; Distribution Unlimited
2b. DECLASSIFICATION/DOWNGRADING SCHEDULE: N/A	
4. PERFORMING ORGANIZATION REPORT NUMBER(S): TR-4423-3	5. MONITORING ORGANIZATION REPORT NUMBER(S): AFGL-TR-85-0066
6a. NAME OF PERFORMING ORGANIZATION: The Analytic Sciences Corp. (6b. OFFICE SYMBOL (If applicable))	7a. NAME OF MONITORING ORGANIZATION: Air Force Geophysics Laboratory
6c. ADDRESS (City, State, and ZIP Code): One Jacob Way, Reading, Mass. 01867	7b. ADDRESS (City, State, and ZIP Code): Hanscom AFB, Mass. 01731
8a. NAME OF FUNDING/SPONSORING ORGANIZATION: Defense Mapping Agency (8b. OFFICE SYMBOL (If applicable))	9. PROCUREMENT INSTRUMENT IDENTIFICATION NUMBER: F19628-83-C-0053
8c. ADDRESS (City, State, and ZIP Code): Washington, D.C. 20305	10. SOURCE OF FUNDING NUMBERS: PROGRAM ELEMENT NO 63701B; PROJECT NO 3201; TASK NO 3201S46; WORK UNIT ACCESSION NO 3201DMAE

11. TITLE (Include Security Classification)
Gravity Gradiometer Survey Errors

12. PERSONAL AUTHOR(S)
Steven J. Brzezowski

13a. TYPE OF REPORT	13b. TIME COVERED	14. DATE OF REPORT (Year, Month, Day)	15. PAGE COUNT
Scientific No. 4	FROM Nov. 84 TO Apr. 85	85 March	38

16. SUPPLEMENTARY NOTATION

17. COSATI CODES		
FIELD	GROUP	SUB-GROUP
08	05	03

18. SUBJECT TERMS (Continue on reverse if necessary and identify by block number)
Gravity, Gravity Survey, Gravity Gradiometer Survey System, Gravity Survey Errors, Statistical Gravity Model

19. ABSTRACT (Continue on reverse if necessary and identify by block number)

Gradiometer system noise, sampling effects, downward continuation and limited data extent contribute to moving-base gravity gradiometer survey error. This report describes the individual effects of these error sources on a gravity gradiometer survey system currently under development. Special techniques are required to account for downward continuation and limited data extent effects which cannot be adequately modeled as measurement noise in a linear error estimation algorithm. The results reported herein indicate the survey performance improvement which could be realized if each error source were totally eliminated. The sensitivity of total survey error to small changes in the nominal value of each error source is also identified.

(Continued)

20. DISTRIBUTION/AVAILABILITY OF ABSTRACT	21. ABSTRACT SECURITY CLASSIFICATION
☐ UNCLASSIFIED/UNLIMITED ☒ SAME AS RPT. ☐ DTIC USERS	UNCLASSIFIED

22a. NAME OF RESPONSIBLE INDIVIDUAL	22b. TELEPHONE (Include Area Code)	22c. OFFICE SYMBOL
Donna L. Warner	617-861-3486	LWG

DD FORM 1473, 84 MAR — 83 APR edition may be used until exhausted. All other editions are obsolete.

SECURITY CLASSIFICATION OF THIS PAGE
UNCLASSIFIED

19. Abstract (Continued)

System performance results are analyzed for several sets of airborne survey conditions. For a typical characterization of the earth's gravity field, limited data extent generally contributes about one-half of the total error variance associated with recovery of the gravity disturbance vector at the earth's surface; gradiometer system noise typically contributes about one-third. However, sampling effects are also very significant (and are controlled through the survey track spacing). The findings of this study indicate that a 5-km track spacing provides a reasonable tradeoff between survey cost and errors due to track spacing and that a moving-base gravity gradiometer system can recover each component of the gravity disturbance vector with an rms accuracy better than 1.0 mGal.

ACKNOWLEDGMENT

The research described in this report was sponsored by the Air Force Geophysics Laboratory and the Defense Mapping Agency under Contract No. F19628-83-C-0053. The author is pleased to acknowledge Dr. Jacob D. Goldstein of The Analytic Sciences Corporation for his formulation of the performance analysis methodology. This methodology is summarized in Appendix B and described in detail in Ref. 1.

TABLE OF CONTENTS

LIST OF FIGURES

LIST OF TABLES

1. INTRODUCTION

1.1 BACKGROUND

Moving-base gravity gradiometry began in earnest during the late 1960s when the Air Force Geophysics Laboratory (AFGL), which was then called Air Force Cambridge Research Laboratories, sought to develop efficient approaches to map the short-wavelength features of the earth's gravity field over large geographical areas. Since the state-of-the-art of gradiometry has been reviewed on previous occasions (Refs. 2, 3), only recent activity in the field will be reviewed here. With steady progress of gravity gradiometer system technology demonstrated, the Defense Mapping Agency (DMA) decided in 1981 to establish a program to produce a new moving-base gradiometer survey system. Under this program, Bell Aerospace Division of Textron, Inc. is developing a Gravity Gradiometer Survey System (GGSS) which is based upon the successfully demonstrated rotating-accelerometer gravity gradiometer concept (Ref. 4).

The GGSS program is being pursued with the goal of gradiometrically surveying the gravity disturbance vector over wide areas to less than 1.0 mGal rms error per component and at high density. In addition, the very rapid data collection rate and anticipated low cost per data unit of surveyed gravity information are sufficiently encouraging to promise widespread use of airborne gradiometers in the future. The GGSS will be capable of deployment in either an aircraft or land vehicle. Of these two options, the recovery of the surface gravity disturbance vector from an aircraft-based GGSS is more difficult and is the problem considered in this report.

The GGSS design consists of a triad of gradiometers mounted on the azimuth (inner) element of a three-axis inertially stabilized platform. As shown in Fig. 1.1-1, the three instruments are symmetrically distributed about the vertical axis, with each gradiometer inclined at the same "umbrella" angle α. Figure 1.1-1 also identifies the u,v,w instrument axes and local-level x,y,z platform axes. Each gradiometer measures two elements of the gravity gradient tensor in the instrument u,v,w coordinate frame, i.e., the cross gradient T_{uv} and the difference of the two in-line gradients, $T_{uu} - T_{vv}$. Mathematical properties of the gravity gradient tensor are reviewed in Appendix A.

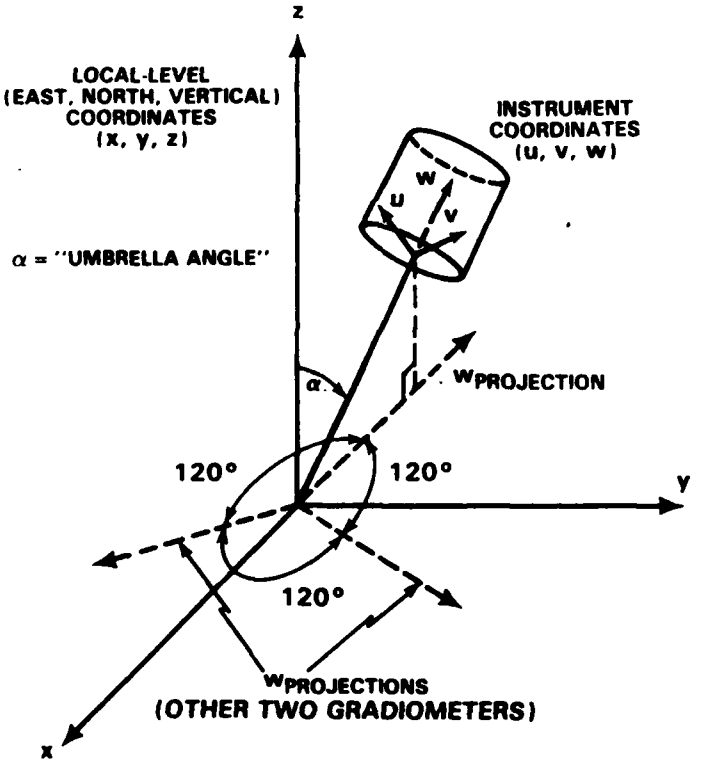

Figure 1.1-1 GGSS Geometry and Coordinate Systems

Earlier works (Refs. 5, 6 and 7) have considered the use of gravity gradiometer data for identifying geologic features to aid oil and mineral exploration. This report refines

the understanding of gradiometer system error sources and provides a basis for both designing gravity field surveys and anticipating the information content (and omission) of the data obtained therefrom.

1.2 GGSS PROGRAM OBJECTIVES

The GGSS is being designed to provide the following accuracies associated with recovery of the short-wavelength (less than 500 km) portion of the gravity disturbance vector when operated as indicated in Fig. 1.2-1 (Ref. 8):

- 0.9 mGal rms error for vertical gravity disturbance
- 0.18 $\widehat{\text{sec}}$ rms error for deflection of the vertical (each axis).

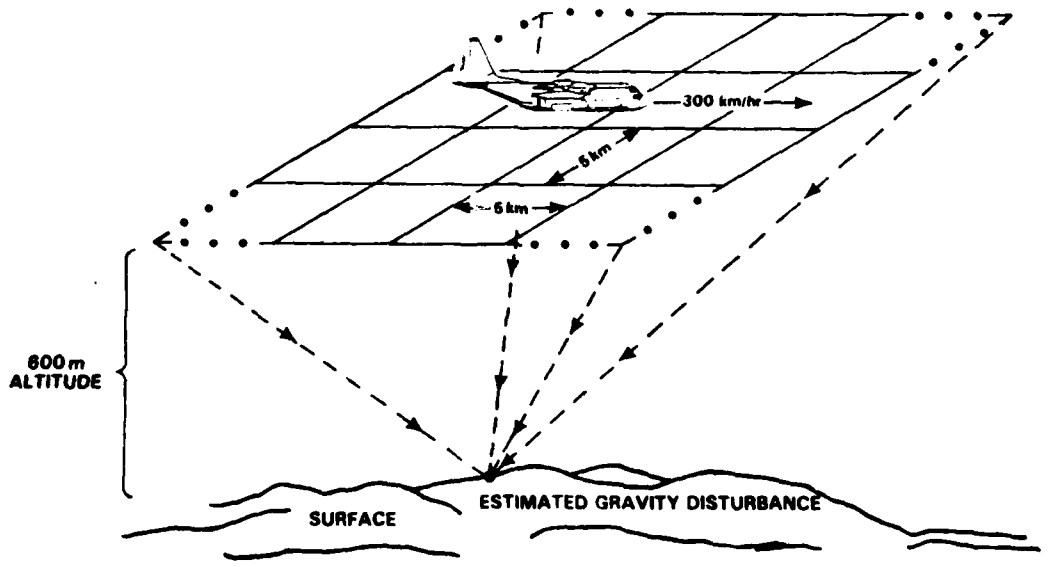

Figure 1.2-1 Nominal GGSS Airborne Survey Parameters

The wavelength specification is imposed only for initial testing to maintain reasonable areal dimensions. In larger surveys, longer wavelength gravity information will be obtained. Using both gradiometer data and long-wavelength gravity information from other sources, the goal for recovery of all wavelengths of the gravity disturbance vector is:

- 1.0 mGal rms error for vertical gravity disturbance
- 0.2 $\widehat{\text{sec}}$ rms error for deflection of the vertical (each axis).

These larger values account for errors in supplemental gravity field data (i.e., sources of long-wavelength gravity information such as the one-deg by one-deg mean anomaly data stored in the DoD Gravity Library at the Defense Mapping Agency Aerospace Center).

2. GGSS ERROR CONTRIBUTORS

2.1 DESCRIPTION OF ERROR SOURCES

GGSS-related errors and survey limitations represent the two fundamental GGSS error source categories. The first refers to inherent characteristics of the gradiometer system, while the second applies to errors associated with the manner in which the survey is operated. A discussion of the individual errors in each category is presented below. Quantitative treatment follows.

GGSS-related errors - Contributors to GGSS-related errors include the following:

- Gradiometer self-generated measurement noise
- Environmentally induced errors
- Navigation, attitude and attitude-rate control uncertainties
- Gimbal, vehicle and nearby-object self-gradient compensation limitations.

Survey limitations - Survey limitations which contribute to airborne GGSS error include sampling effects, downward continuation and limited data extent. These are each summarized below.

When inherently continuous data are sampled, aliasing occurs. This effect represents an error caused by the misrecognition of frequency components higher than one-half of the

sampling frequency. The bi-directional survey traverse pattern, consisting of orthogonal tracks, is required to minimize the effects of cross-track aliasing since no prefiltering is possible in this direction. A well-designed sampling regime and data prefilter are required to minimize potential aliasing errors in the along-track direction.

Downward continuation of measured gravity gradient data from the survey aircraft's altitude is required to estimate gravity disturbance quantities at the earth's surface. As a result, an error due to the loss of the short-wavelength portion of the gravity signal occurs because the gravity gradients associated with highly localized disturbance sources attenuate rapidly with altitude.

Limited data extent reflects the loss of the long-wavelength portion of the gravity gradient signal because the far field is not observed. Thus, this error source is strongly influenced by the overall dimensions of the area which can be traversed.

2.2 DETERMINING THE CONTRIBUTION OF EACH ERROR SOURCE

The procedure selected to evaluate the relative importance of the GGSS error sources consists of comparing the output error when all error sources are acting concurrently (i.e., ordinary situation) with the hypothetical case in which one error source is totally eliminated. By repeating this comparison for each error source, the relative importance of all the error sources can be established. Although this procedure provides an understanding of the major error contributors, it does not offer insight into how small refinements in survey design should be made because of the nonlinear fashion in which

the error sources act. Accordingly, it is also appropriate to compute the sensitivity of total survey error to an incremental change in each error source while maintaining the optimality of the filter (i.e., adjusting the filter to account for geometry redesign). The sensitivity analysis results therefore identify specific factors which provide the most control of gravity disturbance vector recovery accuracy. Using the methodology outlined in Appendix B, the relative ranking and error sensitivities of the GGSS error sources are computed by the following five-step procedure:

1. Determine the nominal rms recovery error with all N error sources present; the notation for this error is σ

2. Compute the rms recovery error if the i^{th} error source is absent; this error is denoted by σ'

3. Compute the contribution of the i^{th} error source acting alone if it is independent of the other error sources and linearly related to the recovery error. This "conditionally independent" contribution is denoted by σ_i and given by

$$\sigma_i = [\sigma^2 - (\sigma')^2]^{\frac{1}{2}} \qquad (2\text{-}1)$$

4. Scale the variance of the i^{th} error source in Step 3 to the sum of variances of all conditionally independent error sources:

$$\text{Percent contribution} = 100 \times \sigma_i^2 \Big/ \sum_{i=1}^{N} \sigma_i^2 \qquad (2\text{-}2)$$

5. Compute the sensitivity of total recovery error to a 10 percent reduction in nominal error variance of each source or as appropriate, a 10 percent reduction in the nominal value of each survey parameter. Applicable survey parameters

are the track spacing, aircraft altitude and survey block size which are all identified in Fig. 1.2-1. This error sensitivity is expressed in terms of a percent change in total error variance.

The above procedure reflects modifications to conventional linear error budget theory which were chosen to account for the nonlinearity in the altitude error term. For this error source, Step 2 above is accomplished by setting the survey altitude parameter h (which explicitly appears in the vector transfer functions listed in Table B-1 of Appendix B) to zero.

The effect of limited data on total post-survey residual error is analyzed in a slightly different fashion from Steps 1-5 for reasons of economy. The contribution of this error source alone is obtained by setting the effects due to GGSS-related errors, sampling and downward continuation to zero and using the optimal error covariance equation:

$$C_{\delta\underline{w},\delta\underline{w}} = C_{\underline{w},\underline{w}} - C_{\underline{w},\underline{z}}\, C^{-1}_{\underline{z},\underline{z}}\, C_{\underline{z},\underline{w}} \,, \qquad (2\text{-}3)$$

where the subscripts $\delta\underline{w}$ and $\underline{z}$ refer to the residual error in the gravity field-related quantities $\underline{w}$ and the observed gradiometer measurements, respectively. Further discussion of these quantities ($\delta\underline{w}$, $\underline{z}$ and $\underline{w}$) is given in Appendix B.

The solution to Eq. 2-3 was implemented using the GEOFAST efficient collocation algorithm (Refs. 9, 10 and 11) which exploits the special structure of the gravity model covariance matrices and uses to advantage the computational efficiency of fast Fourier transforms. The Geodetic Fast Estimation (GEOFAST) algorithm is fully optimal, resulting in

minimum-variance of the estimation error when appropriate gravity models are used. The rms survey error due to the finite extent of the survey was computed using GEOFAST for the case in which no error sources other than finite data extent were acting. The contribution of the finite extent error, computed in this way, was combined with the contributions of the other errors discussed previously using Step 4 in the outlined procedure and root-sum-square addition.

3. RESULTS

This chapter discusses the results of evaluating total post-survey rms residual error caused by the individual error contributors identified in Section 2.1. The results were obtained using the methodology described in Appendix B and the procedures outlined in the previous section. These results are estimates of the accuracy improvement realized by either totally eliminating or incrementally reducing each error source, as discussed earlier.

Error contributions are evaluated using three gravity field models: a "baseline" model which represents a "typical" area that could be surveyed, an "active" model which represents a "geographically rough" area, and a "North Texas" model which represents characteristics particular to the planned GGSS test area. A good representation of the variability of the gravity field is provided by these three models. This allows accurate evaluation of the expected range of variation in GGSS performance. The relationship between these models and actual physiographic features is discussed more fully in Appendix B.

The total rms error associated with recovery of the surface gravity disturbance vector from GGSS data collected at altitude is given in Table 3-1. The sensitivity of these errors to the three different characterizations of the gravity field is indicated. These results are also expressed in terms of the percentage of allowable error based on the GGSS performance specification defined earlier. Note that the results presented in Table 3-1 indicate that the 0.9 mGal rms vertical disturbance accuracy goal is more challenging than the deflection of

TABLE 3-1

SENSITIVITY OF GGSS SHORT-WAVELENGTH (LESS THAN 500 km) RECOVERY TO GRAVITY FIELD MODEL

GRAVITY FIELD MODEL	RMS SURVEY ERROR		ERROR AS A PERCENT OF RMS GGSS SPECIFICATION	
	DEFLECTION OF THE VERTICAL ($\widehat{sec}$)	VERTICAL GRAVITY DISTURBANCE (mGal)	DEFLECTION OF THE VERTICAL (%)	VERTICAL GRAVITY DISTURBANCE (%)
Baseline	0.09	0.7	50	78
North Texas	0.11	0.7	61	78
Active	0.13	0.9	72	100

the vertical goal (0.18 $\widehat{sec}$ rms). This situation is typical for every study case addressed in these analyses and is conjectured to be true in general. For this reason, subsequent discussions emphasize the ability of the GGSS to recover the vertical gravity disturbance quantity. In addition, Table 3-1 shows that gravity disturbances in an area characterized by an active gravity field with unusually large high-frequency content are more difficult to recover than a typical gravity field, such as would be encountered in the North Texas area. The active field corresponds to very rough terrain. Thus, this behavior is expected since rugged terrain causes the gravity disturbance field to possess much more power (e.g., variance) in the frequency range recovered by the gradiometer. As a result, more energy is both aliased (for a given survey track spacing) and lost to downward continuation (for a given survey altitude).

GGSS error contributor rankings and the sensitivities of total GGSS error to each error source are provided in Table 3-2. These results are based on a nominal set of survey operating conditions and error model parameter values as specified in Table 3-3 and explained in Appendix B. The limited extent of

TABLE 3-2

GGSS ERROR CONTRIBUTOR RANKINGS AND SENSITIVITIES
FOR NOMINAL SURVEY CONDITIONS

GRAVITY FIELD MODEL	ERROR SOURCE	PERCENTAGE OF ERROR VARIANCE CONTRIBUTED BY EACH SOURCE	ERROR SENSITIVITY (PERCENT CHANGE IN ERROR VARIANCE)	TOTAL RMS ERROR (mGal)
Baseline	GGSS-Related Errors	34	6.5	0.7
	Survey Limitations			
	• Sampling Effects	12	9.2	
	• Downward Continuation	5	1.7	
	• Limited Data Extent	49	1.9	
North Texas	GGSS-Related Errors	36	3.3	0.7
	Survey Limitations			
	• Sampling Effects	20	7.4	
	• Downward Continuation	9	1.5	
	• Limited Data Extent	35	3.7	
Active	GGSS-Related Errors	37	4.5	0.9
	Survey Limitations			
	• Sampling Effects	30	16.4	
	• Downward Continuation	13	2.8	
	• Limited Data Extent	20	1.4	

TABLE 3-3

NOMINAL SURVEY CONDITIONS AND ERROR MODEL PARAMETER VALUES

PARAMETER	SYMBOL	VALUE	UNITS
Sampling Interval	t_g	10	sec
Track Spacing	t_2	5	km
Survey Altitude	h	600	m
Survey Speed	V	300	km/hr
Survey Block Size	L	500	km
Sensor White Noise Floor	w_k	55	E^2/Hz
Sensor Red Noise Level	r_k	1.7×10^{-4}	$E^2(Hz)$

the survey dominates all other errors for the baseline gravity model case. This is due to the fact that the nominal survey block area simulated in this study is 500 km. As a result, gravity wavelengths longer than about one-half the dimension of the survey region (i.e., about 250 km in this case) are not recovered well. During actual survey operations, some modest improvement in errors induced by limited survey extent is likely since more flight time may be available (i.e., larger areal dimensions will be possible).

The nominal GGSS design parameters, survey along-track sampling time, aircraft altitude, aircraft speed and navigation performance were selected so that their resulting contributions to total survey error would be relatively small for typical gravity field characteristics. The 5-km track spacing was selected as a compromise between short-wavelength gravity field recovery and survey effort as measured in hours of aircraft flight time. Note that in an area involving rough terrain (active gravity field), a significantly larger error contribution results from sampling effects.

Table 3-2 also indicates that, regardless of the type of gravity field which is being surveyed, the greatest benefit to accuracy improvement results from an incremental reduction in the track spacing. This phenomenon is seen by the large error sensitivities associated with sampling effects and is not surprising since decreasing the track spacing provides the most direct mechanism for improving estimates of the high-frequency portion of the gravity field. The findings reported in Table 3-2 indicate that the gradiometer instrument accuracy is sufficient so that, with careful attention to the survey density and areal dimensions, recovery of the gravity disturbance vector will be achievable within specified accuracy levels and reasonable time limits.

4. SUMMARY AND CONCLUSIONS

The GGSS is being developed by Bell Aerospace Textron to collect data for accurately mapping the short-wavelength features of the earth's gravity field over large geographical areas in a relatively quick and inexpensive manner. Detailed consideration of all known error sources which will affect the GGSS indicates that the currently planned system and survey design is adequate to support gravity disturbance vector recovery to within specification.

Among the important effects which contribute to survey inaccuracy are GGSS hardware and system-related errors, sampling effects, downward continuation and limited data extent. Estimation of the post-survey residual rms errors shows that errors due to these effects are somewhat sensitive to the characteristics of the underlying gravity field. More high-frequency content associated with a geographical area to be surveyed (i.e., situations involving rough terrain) leads to larger survey errors. Sampling effects and limited data extent are generally the most significant GGSS error sources. Survey parameters can be selected judiciously so that errors due to these effects are controlled without requiring excessive survey expense. With this careful approach to survey design, components of the gravity disturbance vector can be recovered with better than one mGal rms accuracy.

APPENDIX A
THE GRAVITY GRADIENT TENSOR

Gravitational acceleration $\underline{g}(\underline{r})$ is the spatial derivative of the gravitational potential which is a scalar function T of position $\underline{r}$ from the earth's center. In Cartesian coordinates,

$$\underline{g}(\underline{r}) = [\partial T/\partial x \quad \partial T/\partial y \quad \partial T/\partial z]^T \ , \qquad \text{(A-1)}$$

where the symbol ∂ denotes partial differentiation and the superscript T represents the vector transpose. Using the gradient $\underline{\nabla}$ operator, the gravity gradient tensor $\underline{\Gamma}(\underline{r})$ is the spatial derivative of $\underline{g}(\underline{r})$. In Cartesian coordinates,

$$\underline{\Gamma}(\underline{r}) = \underline{\nabla}\underline{g}(\underline{r}) = \begin{bmatrix} \partial^2 T/\partial x^2 & \partial^2 T/(\partial x \partial y) & \partial^2 T/(\partial x \partial z) \\ \partial^2 T/(\partial y \partial x) & \partial^2 T/\partial y^2 & \partial^2 T/(\partial y \partial z) \\ \partial^2 T/(\partial z \partial x) & \partial^2 T/(\partial z \partial y) & \partial^2 T/\partial z^2 \end{bmatrix} . \qquad \text{(A-2)}$$

Using subscript notation, where the subscripts indicate directional derivatives, Eq. A-2 can be expressed as

$$\underline{\Gamma} = \begin{bmatrix} T_{xx} & T_{xy} & T_{xz} \\ T_{yx} & T_{yy} & T_{yz} \\ T_{zx} & T_{zy} & T_{zz} \end{bmatrix} . \qquad \text{(A-3)}$$

The gravity gradient tensor is symmetric because of the commutativity of mixed partial derivatives (i.e., $T_{ij} = T_{ji}$). In addition, since the gravity field is conservative, Laplace's equation

$$T_{xx} + T_{yy} + T_{zz} = 0 \qquad \text{(A-4)}$$

applies everywhere outside the earth's surface. Thus, complete determination of $\underline{\Gamma}$ at any point requires <u>five</u> independent measurements which mandates the need for three appropriately oriented gradiometers in the GGSS.

APPENDIX B
PERFORMANCE ANALYSIS METHODOLOGY

This appendix outlines the techniques chosen to analyze post-survey residual gravity errors. A frequency-domain approach is used to evaluate the GGSS-related and aliasing measurement error sources. Due to the nonlinear response of survey error to errors caused by downward continuation and limited data extent, a special error allocation treatment (which is described in Chapter 2) is required. Discussion of the two-dimensional frequency-domain approach (Ref. 1) follows.

The problem of determining the total residual error in the estimation of the gravity field from gradiometer survey data can be formulated in general terms as follows. At every point $\underline{x}$ on a planar earth surface, the estimation errors $\delta\underline{w}$ between the true values of the process $\underline{w}$ and the best estimates (in the mean-square sense) $\hat{\underline{w}}$ are given as

$$\delta\underline{w}(\underline{x}) = \underline{w}(\underline{x}) - \hat{\underline{w}}(\underline{x}) \quad . \qquad \text{(B-1)}$$

In the above equation $\underline{x} = (x_1, x_2)^T$ denotes the position of a point on the plane with x_1 and x_2 measured in the east and north directions, respectively. The components of $\underline{w}$ are any collection of gravity field-related quantities.

The estimates $\hat{\underline{w}}$ are optimally obtained from a data set of gradiometer measurements $\underline{z}$ which are linear combinations of gravity gradient quantities $\underline{y}$ corrupted by additive noise $\underline{e}$:

$$\underline{z}(\underline{x}) = \underline{y}(\underline{x}) + \underline{e}(\underline{x}); \; \underline{x} \in M \quad . \qquad \text{(B-2)}$$

In addition, all measurement points ($\underline{x}$) are assumed to form a rectangular grid (M) and the measurement errors are modeled as a stationary Gaussian process independent of the gravity field. (In practice, departures from the grid are allowed. Error models discussed later in the text account for the inaccuracies induced by such departures.)

In general, a linear estimate of $\underline{w}$ is given by

$$\hat{\underline{w}}(\underline{x}) = K(\underline{x})\underline{z} \qquad \text{(B-3)}$$

where all available data on the grid M are used and the estimator K is chosen so that the variance of $\delta\underline{w}(\underline{x})$ is minimized. This estimator is determined from:

- The types of data collected (e.g., gravity gradients) and the relation of these data to the quantities being estimated
- The physical characteristics of the survey (e.g., track spacing, time interval between samples, etc)
- A statistical model for the gravity field
- Statistical models for the measurement noise corrupting the data.

The analysis of the post-survey residual errors $\delta\underline{w}$ is performed in the frequency domain using multi-dimensional Wiener filtering. The statistics of these errors at any given point depend upon the relative position of the point with respect to the measurements and are computed in the form of power spectral densities (PSDs). The spectral density of $\delta\underline{w}$ is the Fourier transform of its auto-covariance and is given by

$$\phi_{\delta\underline{w},\delta\underline{w}}(\underline{s}) = \phi_{\underline{w},\underline{w}}(\underline{s}) - \hat{K}(s)\,\phi_{\underline{z},\underline{w}}(\underline{s}) \quad , \qquad \text{(B-4)}$$

where

$$\underline{s} = (s_1, s_2)^T \qquad \text{(B-5)}$$

with s_1 and s_2 being spatial frequencies measured in the east and north directions, respectively. The Fourier transform of the optimal estimator $\hat{K}$ can be expressed in terms of the spectral densities of the measurement and estimated processes by

$$\hat{K}(\underline{s}) = \phi_{\underline{w},\underline{z}}(\underline{s})\ \phi^{-1}_{\underline{z},\underline{z}}(\underline{s}) \quad . \qquad \text{(B-6)}$$

Since,

$$\phi_{\underline{z},\underline{w}}(\underline{s}) = \phi^{\#}_{\underline{w},\underline{z}}(\underline{s}) \quad , \qquad \text{(B-7)}$$

where # indicates complex conjugate transpose, Eq. B-4 can be rewritten as

$$\phi_{\delta\underline{w},\delta\underline{w}} = \phi_{\underline{w},\underline{w}} - \phi_{\underline{w},\underline{z}}\ \phi^{-1}_{\underline{z},\underline{z}}\ \phi^{\#}_{\underline{w},\underline{z}} \quad . \qquad \text{(B-8)}$$

Taking into account the independence of the gravity field and measurement errors, it follows that

$$\phi_{\underline{w},\underline{z}} = \phi_{\underline{w},\underline{y}} \quad . \qquad \text{(B-9)}$$

In addition, Eq. B-2 can be expressed in terms of spectral densities as

$$\phi_{\underline{z},\underline{z}} = \phi_{\underline{y},\underline{y}} + \phi_{\underline{e},\underline{e}} \quad . \qquad \text{(B-10)}$$

Therefore, substituting Eqs. B-9 and B-10 into B-8 yields

$$\Phi_{\delta\underline{w},\delta\underline{w}} = \Phi_{\underline{w},\underline{w}} - \Phi_{\underline{w},\underline{y}} \left[\Phi_{\underline{y},\underline{y}} + \Phi_{\underline{e},\underline{e}}\right]^{-1} \Phi^{\#}_{\underline{w},\underline{y}} \quad . \qquad \text{(B-11)}$$

The estimated variables $\underline{w}$ and measured quantities $\underline{y}$ are related to the anomalous surface potential T_o through vector transfer functions $\underline{G}$ and $\underline{F}$ as follows:

$$\Phi_{\underline{w},\underline{w}} = \underline{G}\ \underline{G}^{\#}\ \Phi_{T_o,T_o} \qquad \text{(B-12)}$$

$$\Phi_{\underline{y},\underline{y}} = \underline{F}\ \underline{F}^{\#}\ \Phi_{T_o,T_o} \qquad \text{(B-13)}$$

$$\Phi_{\underline{w},\underline{y}} = \underline{G}\ \underline{F}^{\#}\ \Phi_{T_o,T_o} \quad , \qquad \text{(B-14)}$$

where Φ_{T_o,T_o} is the PSD of the unsurveyed surface anomalous potential obtained from a gravity field model, such as those discussed later in this appendix. Appropriate expressions for the vector transfer functions $\underline{G}$ and $\underline{F}$ are obtained from the entries given in Table B-1.

The spectral density of the post-survey residuals in $\underline{w}$ is obtained from a similar expression, namely

$$\Phi_{\delta\underline{w},\delta\underline{w}} = \underline{G}\ \underline{G}^{\#}\ \Phi_{\delta T_o,\delta T_o} \quad , \qquad \text{(B-15)}$$

where the ensemble spectral density of the residual surface anomalous potential is given by

$$\Phi_{\delta T_o,\delta T_o} = 1 \Big/ \left[\underline{F}^{\#}\ \Phi^{-1}_{\underline{e},\underline{e}}\ \underline{F} + 1/\Phi_{T_o,T_o}\right] \quad , \qquad \text{(B-16)}$$

and where $\Phi_{\underline{e},\underline{e}}$ is the spectral density matrix of the measurement errors. The vector transfer function $\underline{G}$ must also take into account the transformation between the gradiometer instrument frame and the desired geodetic east, north, vertical (x,y,z) frame. As noted earlier, each of the two gradiometer

TABLE B-1

TRANSFER FUNCTIONS FROM ANOMALOUS SURFACE POTENTIAL

QUANTITY	SYMBOL*	RELATION TO ANOMALOUS POTENTIAL	TRANSFER FUNCTION FROM ANOMALOUS SURFACE POTENTIAL†
Anomalous Potential at Height h	T_h	T_h	$e^{-2\pi sh}$
East Component of Gravity Disturbance Vector at Height h	T_x	$\partial T_h/\partial x$	$i2\pi s_1 e^{-2\pi sh}$
North Component of Gravity Disturbance Vector at Height h	T_y	$\partial T_h/\partial y$	$i2\pi s_2 e^{-2\pi sh}$
Vertical Component of Gravity Disturbance Vector at Height h	T_z	$\partial T_h/\partial z$	$-2\pi s e^{-2\pi sh}$
East-East Gradient at Height h	T_{xx}	$\partial^2 T_h/\partial x^2$	$-4\pi^2 s_1^2 e^{-2\pi sh}$
North-North Gradient at Height h	T_{yy}	$\partial^2 T_h/\partial y^2$	$-4\pi^2 s_2^2 e^{-2\pi sh}$
Vertical-Vertical Gradient at Height h	T_{zz}	$\partial^2 T_h/\partial z^2$	$4\pi^2 s^2 e^{-2\pi sh}$
East-North Gradient at Height h	T_{xy}	$\partial^2 T_h/(\partial x \partial y)$	$-4\pi^2 s_1 s_2 e^{-2\pi sh}$
East-Vertical Gradient at Height h	T_{xz}	$\partial^2 T_h/(\partial x \partial z)$	$-i4\pi^2 s_1 s e^{-2\pi sh}$
North-Vertical Gradient at Height h	T_{yz}	$\partial^2 T_h/(\partial y \partial z)$	$-i4\pi^2 s_2 s e^{-2\pi sh}$

*x,y,z corresponds to an east, north, vertical geodetic coordinate frame

†$s = (s_1^2 + s_2^2)^{1/2}$; $i = \sqrt{-1}$.

outputs measures a certain linear combination of the gradients of the potential. This combination is given by the following relation:

$$\begin{bmatrix} T_{11} \\ T_{12} \\ T_{21} \\ T_{22} \\ T_{31} \\ T_{32} \end{bmatrix} = \begin{bmatrix} -1/4 & 1/4 & 0 & \sqrt{3}/6 & \sqrt{2}/2 & \sqrt{6}/6 \\ -1/3 & 0 & 1/3 & -\sqrt{3}/3 & -\sqrt{2}/6 & \sqrt{6}/6 \\ 1/4 & -1/4 & 0 & \sqrt{3}/6 & -\sqrt{2}/2 & \sqrt{6}/6 \\ -1/3 & 0 & 1/3 & \sqrt{3}/3 & -\sqrt{2}/6 & -\sqrt{6}/6 \\ 0 & 0 & 0 & -\sqrt{3}/3 & 0 & -\sqrt{6}/3 \\ 1/6 & -1/2 & 1/3 & 0 & \sqrt{2}/3 & 0 \end{bmatrix} \begin{bmatrix} T_{xx} \\ T_{yy} \\ T_{zz} \\ T_{xy} \\ T_{xz} \\ T_{yz} \end{bmatrix} , \tag{B-17}$$

where T_{ij} represents the j^{th} output of the i^{th} gradiometer ($j = 1,2$ and $i = 1,2,3$) and T_{xx}, T_{yy}, T_{zz}, T_{xy}, T_{xz} and T_{yz} are elements of the gravity gradient tensor (see Eq. A-3) in an east (x), north (y), up (z) reference frame.

The inverse Fourier transform of $\phi_{\delta\underline{w},\delta\underline{w}}$ yields the covariance matrix of the residuals:

$$R_{\delta\underline{w},\delta\underline{w}}(\underline{x}) = \int_{-\infty}^{\infty}\int_{-\infty}^{\infty} \phi_{\delta\underline{w},\delta\underline{w}}(\underline{s})\, e^{i2\pi\langle\underline{x},\underline{s}\rangle}\, ds_1\, ds_2 \quad , \tag{B-18}$$

where

$$\langle\underline{x},\underline{s}\rangle = x_1 s_1 + x_2 s_2 \tag{B-19}$$

is the scalar product of the vectors $\underline{x}$ and $\underline{s}$. The rms values of the residuals in the components of $\underline{w}$ are obtained by taking square roots of the diagonal elements of the matrix resulting from Eq. B-18, evaluated at $\underline{x} = 0$.

Equation B-16 is the fundamental formula for evaluating post-survey residual rms errors. From this equation, spectral densities and covariances of the residual errors in

the estimation of the gravity field from GGSS measurements are obtained after using Eqs. B-15 and B-18.

The spectral density of the measurement errors, whose inverse appears in Eq. B-16, is given by

$$\phi_{\underline{e},\underline{e}} = \phi_1 + \phi_2 \quad , \tag{B-20}$$

where ϕ_1 and ϕ_2 represent the PSDs of the GGSS-related and sampling effects measurement error sources, respectively. The measurement error spectral density matrix ϕ_1 is diagonal. Entries along the diagonal of ϕ_1 are given by

$$\phi_1(k,k) = m_k + n_k \tag{B-21}$$

for $-1/(2\tau_1) < s_1 < 1/(2\tau_1)$, $k = 1,2,\ldots,6$ and with

$$m_k = \tau_2 \, V \, w_k \tag{B-22}$$

$$n_k = \tau_2 \, (2\pi)^{1.6} \, r_k/(V \, w_1^{1.6}) \tag{B-23}$$

where τ_2 is the track-spacing parameter, V is the speed of the aircraft carrying the GGSS, w_k and r_k are the white noise floor and red noise level of the GGSS time spectra (Ref. 12) and $w_1 = 2\pi s_1$. In addition, τ_1 represents the along-track sampling interval given by

$$\tau_1 = t_g V \tag{B-24}$$

with t_g being the time interval between samples. The nominal values for these parameters are given in Table 3-3. (The values given in Table 3-3 for w_k and r_k relate to a double-sided

PSD formulation; the values for a single-sided PSD formulation are 17.5 E^2 (rad/sec) and 1.0×10^{-3} E^2/rad/sec, respectively.)

For computational purposes, the aliasing contribution, ϕ_2, is conveniently obtained directly from the spectral density of the unsurveyed anomalous surface potential, ϕ_{T_o,T_o}, using the expression

$$\phi_2 = \sum_{\underline{\Lambda}\neq\underline{0}} \underline{F}(\underline{s}+\theta J^{-1}\underline{\Lambda})\underline{F}^{\#}(\underline{s}+\theta J^{-1}\underline{\Lambda})\phi_{T_o,T_o}(\underline{s}+\theta J^{-1}\underline{\Lambda}), \quad \text{(B-25)}$$

where $\underline{\Lambda} = (\ell,m)^T$ is a vector with integer components. In general, it is sufficient to only use the terms corresponding to the values of $\underline{\Lambda}$ given by

$$\underline{\Lambda}|\underline{\Lambda} \neq \underline{0},\ ||\underline{s} + \theta J^{-1}\underline{\Lambda}|| < 2||\underline{s}'|| \quad \text{(B-26)}$$

where $\underline{s}'$ is the vector of Nyquist frequencies associated with the survey and $||\cdot||$ denotes vector magnitude. In Eq. B-25 θ represents a rotation matrix determined by the orientation, α, of the survey tracks relative to the east direction and is defined by

$$\theta = \begin{bmatrix} \cos\alpha & -\sin\alpha \\ \sin\alpha & \cos\alpha \end{bmatrix}; \quad \text{(B-27)}$$

J represents a spacing matrix determined by the separation between survey tracks (τ_2) and between samples along a track (τ_1) and is defined by

$$J = \begin{bmatrix} \tau_1 & 0 \\ 0 & \tau_2 \end{bmatrix}. \quad \text{(B-28)}$$

A stationary gravity field model can be completely specified by the spectral density of the anomalous surface potential, Φ_{T_o,T_o}. Spectral densities, covariances and cross-covariances of all other geodetic quantities can be derived from Φ_{T_o,T_o} using frequency-domain techniques and appropriate transfer functions (see Table B-1). Important features of the baseline, active and North Texas gravity field models used to obtain the results given in this report are provided below.

The baseline and active models each consists of the sum of two third-order Markov stationary random processes along a single track. An individual third-order Markov model (Ref. 13) has a surface potential with a spectral density of the form

$$\Phi^{(k)}(\underline{s}) = 10\pi\ \sigma_k^2\ \beta_k^5/[\beta_k^2 + (2\pi s)^2]^{7/2} \qquad \text{(B-29)}$$

where $1/\beta_k$ is the characteristic distance, σ_k^2 is the variance of the surface potential, and the magnitude of $\underline{s}$ is given by

$$s = (s_1^2 + s_2^2)^{1/2} \quad . \qquad \text{(B-30)}$$

For both the baseline and active models

$$\Phi_{T_o,T_o}(\underline{s}) = \sum_{k=1}^{2} \Phi^{(k)}(\underline{s}) \qquad \text{(B-31)}$$

with $\Phi^{(k)}$ as defined in Eq. B-29. The parameters of the baseline and active models were obtained by fitting to data from the North Atlantic and Bonin Trench, respectively. These parameters are given in Table B-2. The models have been related to

land gravity data as well. On land, the baseline model corresponds to the gravity field of moderate terrain; the active model corresponds to very mountainous terrain.

TABLE B-2
BASELINE AND ACTIVE GRAVITY MODEL PARAMETERS

MODEL	k	$1/\beta_k$ (km)	σ_k $(m/s)^2$
Baseline	1	27.78	16.00
	2	370.4	91.43
Active	1	22.22	29.98
	2	350.03	103.68

The North Texas model (Ref. 14) is a flat-earth Attenuated White Noise (AWN) gravity model (Ref. 15) which describes the proposed GGSS test area. A single shell of an AWN model contributes a surface potential with spectral density

$$\phi^{(k)}(\underline{s}) = 8\pi\, D_k^2\, \sigma_k^2\, e^{-4\pi D_k s} \qquad \text{(B-32)}$$

which can be viewed as resulting from a spherical shell at depth D_k below the surface of the earth on which the potential is white and such that the surface potential has variance σ_k^2. The complete North Texas AWN model consists of seven independent shells, such that

$$\phi_{T_o,T_o}(\underline{s}) = \sum_{k=1}^{7} \phi^{(k)}(\underline{s}) \qquad \text{(B-33)}$$

with $\phi^{(k)}$ as defined in Eq. B-32. The model was fitted to all worldwide and local gravity-field information which is applicable to the GGSS test site. The resulting (flat-earth) model parameters are given in Table B-3.

TABLE B-3
NORTH TEXAS GRAVITY MODEL PARAMETERS

SHELL (k)	D_k (km)	σ_k^2 $(m/s)^2$
1	2.1	0.023
2	5.0	0.11
3	16	0.72
4	52	5.8
5	161	23
6	861	70
7	2150	330

Since the active model contains a substantial amount of high-frequency energy, it is not surprising that it applies to areas with strong physiographic features such as mountain ranges, escarpments and ocean trenches. Alternatively, the baseline model, which contains a moderate amount of both high-frequency and low-frequency energy, best characterizes areas containing more typical physiographic features such as plains, shelfs and basins. The North Texas model is an intermediate type model which is appropriate for the physiography existing in northern Texas. For comparison purposes, the rms values of the gravity anomaly and deflections of the vertical for each of these models are listed in Table B-4.

TABLE B-4

RMS VALUES OF GRAVITY MODEL QUANTITIES

QUANTITY	UNITS	BASELINE MODEL	ACTIVE MODEL	NORTH TEXAS MODEL
Gravity Anomaly	mGal	51.1	112.5	31.3
Deflection of the Vertical (each axis)	$\widehat{sec}$	7.6	16.8	4.7
East-East Gradient	E	20.7	60.6	13.0
North-North Gradient	E	20.7	60.6	13.0
Vertical-Vertical Gradient	E	33.8	99.0	21.2
East-North Gradient	E	12.0	35.0	7.5
East-Vertical Gradient	E	23.9	70.0	15.0
North-Vertical Gradient	E	23.9	70.0	15.0

REFERENCES

1. Goldstein, J.D., "Analysis and Simulation of Multisensor Gravity Surveys," The Analytic Sciences Corporation, Air Force Geophysics Laboratory Report No. AFGL-TR-81-0018(I), December 1980 (Revised March 1985), ADA-160388.

2. Williams, O.W., "Gradiometry -- an Assessment of the State-of-the-Art," Seventh International Gravity Commission Meeting, Paris, France, September 1974.

3. Heller, W.G., "Developments in Moving-Base Gradiometry," Eighth International Gravity Commission Meeting, Paris, France, September 1978.

4. Metzger, E.H., "Development Experience of Gravity Gradiometer System," IEEE Position Location and Navigation Symposium, Atlantic City, NJ, December 1982.

5. Hammer, S., and Anzoleaga, R., "Exploring for Stratigraphic Traps with Gravity Gradients," Geophysics, Vol. 40, No. 2, April 1975, pp. 256-268.

6 Stanley, J.M., and Green, R., "Gravity Gradients and the Interpretation of the Truncated Plate," Geophysics, Vol. 41, No. 6, December 1976, pp. 1370-1376.

7. Gupta, V.K., and Ramani, N., "Optimum Second Vertical Derivatives in Geologic Mapping and Mineral Exploration," Geophysics, Vol. 47, No. 12, December 1982, pp. 1706-1715.

8. Jekeli, C., "Accuracy Specifications of AFGL's Airborne Gravity Gradiometer Survey System," American Geophysical Union Spring Meeting, Baltimore, MD, June 1983.

9. Heller, W.G., Tait, K.S., and Thomas, S.W., "GEOFAST -- a Fast Gravimetric Estimation Algorithm," The Analytic Sciences Corporation, Air Force Geophysics Laboratory Report No. AFGL-TR-77-0195, August 1977, ADA-047611.

10. Tait, K.S., "A Fast Estimation Algorithm for Two-Dimensional Gravity Data (GEOFAST)," The Analytic Sciences Corporation, Air Force Geophysics Laboratory Report No. AFGL-TR-80-0016, November 1979, ADA-086835.

11. Tait, K.S., "A Generalized Fast Estimation Algorithm for Geodetic Applications," The Analytic Sciences Corporation, Technical Report TR-1946-7, December 1982.

REFERENCES (Continued)

12. White, J.V., "Error Models for Gravity Gradiometers in Airborne Surveys," The Analytic Sciences Corporation, Air Force Geophysics Laboratory Report No. AFGL-TR-80-0220, January 1980, ADA-097745.

13. Baumgartner, S.L., Capp, D.W., and Heller, W.G., "Assessment of Inertial Technology for Gravity Survey Applications," The Analytic Sciences Corporation, U.S. Army Report No. ETL-0291-1, May 1982.

14. White, J.V., "A Statistical Gravity Model for Northern Texas," The Analytic Sciences Corporation, Air Force Geophysics Laboratory Report No. AFGL-TR-85-0037, November 1984.

15. Heller, W.G., and Jordan, S.K., "Attenuated White Noise Statistical Gravity Model," Journal of Geophysical Research, Vol. 84, No. B9, August 1979, pp. 4680-4688.

END

FILMED

4-86

DTIC